COBEM UBERLÂNDIA 2019

ABCM Associação Brasileira de Engenharia e Ciências Mecânicas

25th ABCM International Congress of Mechanical Engineering
October 20-25, 2019, Uberlândia, MG, Brazil

COMMAND AUTOMATIZATION OF AN AR.DRONE QUADROTOR FOR PERFORMING INDOOR FLIGHTS

Marcos Antonio Gomes da Silva[1]
Waltencir dos Santos Andrade[2]
Josiel Alves Gouvêa[2]
Alessandro Rosa Lopes Zachi[1]
Centro Federal de Educação Tecnológica Celso Suckow da Fonseca - CEFET/RJ.
[1]Campus Maracanã - Avenida Maracanã 229, Bairro Maracanã , 20.271-110 - Rio de Janeiro - RJ, Brazil.
[2]Campus Nova Iguaçu - Estrada de Adrianópolis 1317, Bairro Santa Rita, 26.041-271 - Nova Iguaçu - RJ, Brazil.
marcosgi7@yahoo.com.br; waltencir.andrade@cefet-rj.br; josiel.gouvea@cefet-rj.br; alessandro.zachi@cefet-rj.br

Abstract. *This work describes the automatization of flight commands of a quadrotor-type Unmanned Aerial Vehicle (AUV). In the developments, a low cost and commercialy available Parrot AR.Drone 2.0 quadrotor model is adopted. The key idea is to take advantages of the drone's internal hardware controller and sensors, in order to design a stable automatic controller. The main objective of the present approach is to use the theory of Active Disturbance Rejection Control (ADRC) method for computing the external flight commands automatically (i.e., without user intervention) and send them to the quadrotor's microcontroller board. An attractive property of the ADRC method is its robustness against parametric uncertainties and unmodeled dynamics of the system. The controller performance is illustrated via simulation and experimental results.*

Keywords: *Quadrotor, UAV, robust ADRC control, indoor flight, AR.Drone 2.0*

1. INTRODUCTION

The attitude control of Unmanned Aerial Vehicles (UAVs) has been an issue of intense research in the last decades. In particular, the four-rotor UAV, which is commonly known as the quadrotor, has gained popularity due to its application in military and civilian fields. Advances in the mechanism fabrication and novel electronics solutions, such as, the navigation sensors, the remote control circuits and power storage systems, have made possible the development of a wide range drone models which can be utilized in several situations for aiding human on difficult tasks. In fact, because of its ability of performing vertical take-off, landing, hover and of possessing great flight maneuvers agility, it has been considered as a potential tool in several relevant applications such as surveillance (Kim *et al.*, 2017), (Lee and Song, 2018), agriculture (Berni *et al.*, 2009), (Hernandez *et al.*, 2015), (Yin *et al.*, 2018), inspection (Máthé *et al.*, 2016), military (Bednowitz *et al.*, 2014), (Feng *et al.*, 2017) and entertainment (Kim *et al.*, 2018).

2. PROBLEM STATEMENT

In the present work, the problem of controlling a quadrotor UAV for performing predefined indoor flight is considered. The central idea is to use the commercially available model with an external automatic controller for replacing the user manual commands. The main motivation for developing efficient control schemes for such vehicles is that the quadrotor UAV is a complex and challenging dynamical system. In addition to the nonlinearities of the mathematical model, the system also presents coupling among control variables and exhibits underactuated behavior. In the present approach, a Parrot AR.Drone 2.0 quadrotor aerial vehicle is used (Bristeau *et al.*, 2011), as illustrated in Fig. 1. This low cost market model comes with an internal flight controller that uses data from inertial sensors as feedback information. It is composed of two pairs of brushless DC motors which are the actuators responsible for the flight maneuvers. Additionally, it has a rechargeable battery pack which may allow a continuous flight of about 12 minutes, and a Wi-Fi communication module which allows remote human manual operation through smartphones and tablets. In order to perform safe movements of take-off, landing and hover, an internal firmware is installed on its microcontroller main board for allowing it to execute the commands sent by the user. The main challenge of dealing with the AR.Drone 2.0 model is the lack of access to the internal flight control parameter.

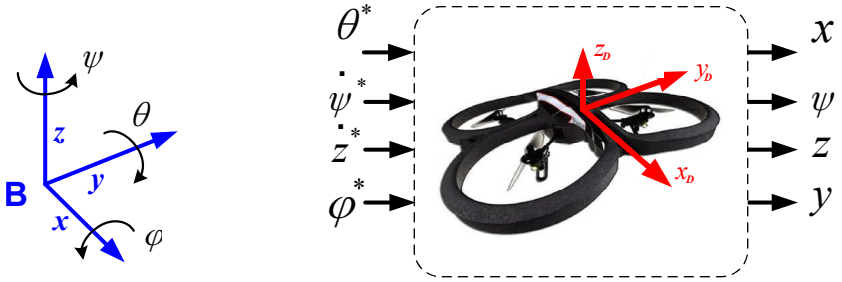

Figure 1: The coordinated systems and input/output variables for the AR.Drone 2.0 vehicle.

2.1 Related works and proposed methodology

Once the internal controller hardware possesses well adjusted parameters from fabric, the quadrotor overall dynamics behaves like a *Linear Time-Invariant System*, seeing from the user set-point commands to the system outputs variables x, y, z and ψ. By regarding such behavior, several control techniques have already been applied recently. In (Babu *et al.*, 2017), a gradient descent based self tuning PID controller has been developed for AR.Drone quadrotors. The authors used the method of Pseudo-Random Binary Signal (PRBS) to identify the system dynamics of each degree of freedom, which resulted in four uncoupled linear transfer functions. In (Merheb *et al.*, 2017), it is proposed an emergency controller that operates in the case of rotor failure. The proposed controller uses the same proportional-integral-derivative (PID) used by the quadrotor, but with an algorithm for redistributing its control signals among the remaining fault-free rotors.

2.2 A brief review about the ADRC method

As can be seen from the generalization formalisms adopted in several works (Zheng *et al.*, 2007), (Zheng *et al.*, 2008), (Madoński *et al.*, 2015), (Xia *et al.*, 2016), (Guo *et al.*, 2017), (Xia *et al.*, 2018), (Zachi *et al.*, 2019), the ADRC paradigm provides a control design methodology that is suitable for large classes of linear and nonlinear systems. The idea proposed by the basic ADRC method is to generate estimates of the non measurable signals of the plant by using an Extended State Observer (ESO) (Madoński *et al.*, 2015) and use those estimates to generate the control law for the system (Han, 2009), (Xia *et al.*, 2016), (Guo *et al.*, 2017), (Xia *et al.*, 2018). The main characteristics of the ADRC method are simpler implementation and good robustness properties against external disturbance, unmodeled dynamics and parametric uncertainties.

According to the recent works involving ADRC paradigm (Madoński *et al.*, 2015), (Xia *et al.*, 2016), (Guo *et al.*, 2017), (Xia *et al.*, 2018), plant uncertainties are taken into account in the control design, with the exception of the control gain, which is considered known. However, in many practical applications, such as load transport by mobile robots and/or drones, the value of the load mass may vary during task execution. In such situation, an uncertainty in the control gain may arise because the mass and inertia parameters of the system mathematical model depend on the value of the load mass. Since this sort of uncertainty affects the amplitude of the control signal and/or its direction, a more careful attention should be focused for this issue.

In the present approach, the key idea is to use the modified version of Active Disturbance Rejection Control (ADRC) method proposed by Zachi *et al.* (2019) for computing the external flight commands automatically (i.e., without user intervention) and send them to the quadrotor's microcontroller board. Illustrative block diagrams of the basic and modified ADRC methods are shown in Fig. 2.

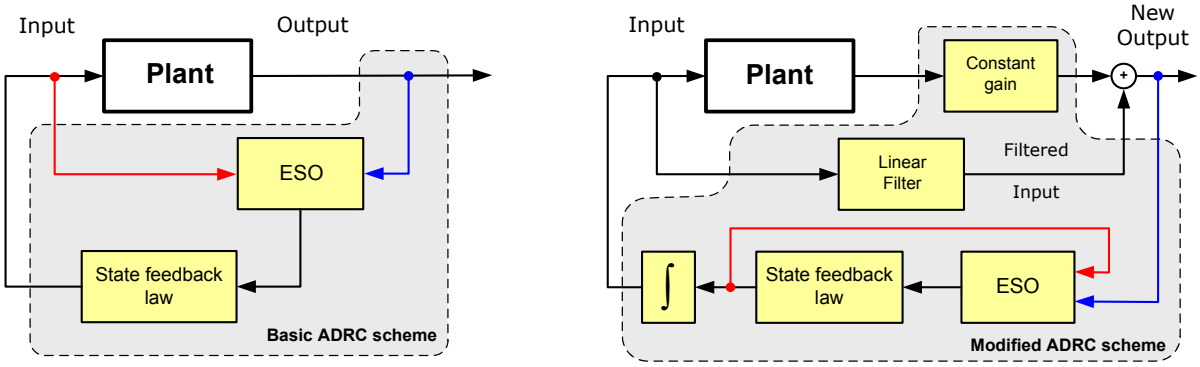

Figure 2: Block diagram of the basic and modified ADRC schemes.

2.3 Basic ADRC development

As a general introduction, let us consider the control design for a general class of n-th order dynamical systems (plants) that can be represented in the following form:

$$y^{(n)} = f\big(Y, d(t), h(Y)\big) + bu(t)\,, \tag{1}$$

$$Y(t) = [y,\ \dot{y},\ \cdots,\ y^{(n-1)}]^T\,, \tag{2}$$

in which $y(t) \in \mathbb{R}$ is the output variable, $u(t) \in \mathbb{R}$ is the input variable, $d(t) \in \mathbb{R}$ is an external disturbance, $Y \in \mathbb{R}^n$ is the system state vector, $b \in \mathbb{R}$ is a constant that will be denoted by the input *control gain*, and $h(Y) \in \mathbb{R}$ represents a nonlinear function of the state variables. We use the notation $y^{(n)}$ to represent the n-th order time derivative of $y(t)$. The function $f(Y, d(t), h(Y))$ in (1) is usually denoted in the literature by the plant *total disturbance* term (Han, 2009), (Madoński *et al.*, 2015). For simplicity, we shall henceforth denote $f(Y, d(t), h(Y))$ by $f(t)$. The control objective is to force the plant output $y(t)$ to track a desired, bounded, trajectory $y^*(t) \in \mathbb{R}$, at least asymptotically, by designing a stable control law for $u(t)$. From input/output point of view, the plant represented by (1) can be considered as a n-th order integrator system with an input $u(t)$, an output $y(t)$ and an input disturbance $f(t)$ in standard form, as depicted in Fig. 3.

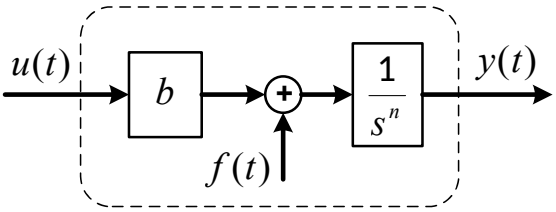

Figure 3: Block diagram of the plant (1) using ADRC formalism.

In the basic ADRC scheme discussed in references (Han, 2009), (Madoński *et al.*, 2015), the control input to be applied to Eq.(1) is designed as:

$$u(t) = u^*(t) = \left(\frac{1}{b}\right)\Big[-f(t) - \lambda_1\dot{y} - \lambda_0(y - y^*)\Big]\,, \tag{3}$$

in which $u^*(t) \in \mathbb{R}$ is a special notation for the ideal control law expression and, $\lambda_1, \lambda_0 \in \mathbb{R}$ are the constant coefficients of a stable and monic polynomial of order 2. In general case, $f(t)$ and the higher order derivatives of $y(t)$ are non available signals. Then, in this case, the ADRC methodology proposes a control law that is computed by using estimates of such quantities, namely,

$$u(t) = \left(\frac{1}{b}\right)\Big[-\hat{f}(t) - \lambda_1\dot{\hat{y}} - \lambda_0(\hat{y} - y^*)\Big]\,, \tag{4}$$

that are all generated by an extended state observer (ESO).

2.4 Modified ADRC approach

In order to deal with the uncertainties that may occur in the control coefficient b of Eqs. (1), a modified framework (Zachi *et al.*, 2019) is proposed for the ADRC scheme of the previous Section. The main contribution of the proposal of Zachi *et al.* (2019) is to introduce a structural transformation in the input/output description of the original system, aiming to obtain a new dynamical equation with known control coefficient (gain). Once it has been achieved, then the ADRC method will be applied without restrictions. As can be observed from Fig.2, the proposed modifications are the insertion of a constant gain block in series with the plant output and the insertion of a linear filter block in parallel with them. Thus, as a consequence, the time domain description of the resulting system remains with a control term with unitary coefficient, which does not impose any restrictions to the designs of the control law and of the ESO.

3. SYSTEM DESCRIPTION

For driving the AR.Drone 2.0 vehicle, the user needs to feed the internal controller with set-point inputs values for θ (pitch angle), ϕ (roll angle), $\dot{\psi}$ (yaw angular velocity) and $\dot{z}$ (vertical linear velocity) (Hernandez *et al.*, 2015), (Babu *et al.*, 2017), as can be observed from the schematic of Fig. 1. This can be accomplished, manually, by maneuvering a joystick console or by pressing buttons in a touchpad device. In the present proposal, such set-point inputs for the drone internal controller are dynamically generated by an ADRC strategy, automatically.

Modeling: For describing the general flight behavior of a quadrotor UAV in terms of translational and rotational movements, one may adopt the classical nonlinear dynamical equations that are available in literature (Kim *et al.*, 2009), (Merheb *et al.*, 2017). However, since we aim to generate the reference values for the input variables θ, ϕ, $\dot{\psi}$ and $\dot{z}$, we only need to consider the simplified version of the drone dynamical equations. Such simplifying assumptions do not cause lost of generality of the ADRC controller because of its well known properties of robustness to unmodeled dynamics and/or to parametric uncertainties of the model (Madoński *et al.*, 2015), (Riveros *et al.*, 2017). Then, for designing purpose, by assuming sufficiently small pitch (θ) and roll (ϕ) angles in the model discussed in (Merheb *et al.*, 2017), we have that:

$$
\begin{array}{ll}
Simplified\ version: & Version\ for\ designing\ purpose: \\
\begin{cases}
\ddot{x} \approx \frac{U_1}{m}(\phi\, s\psi + \theta\, c\psi)\,, \\
\ddot{y} \approx \frac{U_1}{m}(-\phi\, c\psi + \theta\, s\psi)\,, \\
\ddot{z} \approx -\frac{U_1}{m} + g\,, \\
\ddot{\psi} \approx \frac{U_4}{I_z}
\end{cases}
&
\begin{cases}
\ddot{x} = \frac{U_1}{m}(\phi^*\, s\psi + \theta^*\, c\psi)\,, \\
\ddot{y} = \frac{U_1}{m}(-\phi^*\, c\psi + \theta^*\, s\psi)\,, \\
\dot{z} = \dot{z}^*\,, \\
\dot{\psi} = \dot{\psi}^*\,,
\end{cases}
\end{array}
\tag{5}
$$

in which $x,\ y,\ z\ \in \mathbb{R}\ [meters]$ are the spatial coordinates of the quadrotor with respect to the base frame B (Fig. 1), $\phi,\ \theta, \psi\ \in \mathbb{R}\ [rad]$ are the roll, pitch, and yaw orientation angles of the quadrotor, respectively, and $\mathbf{U} = [U_1\ U_2\ U_3\ U_4]^T$ is the vector of control signals which are formed by combination of quadratic functions of the rotors' speeds $\Omega_1,\ \Omega_2,\ \Omega_3, \Omega_4$ and of drag and thrust coefficients. The constant parameters $I_x,\ I_y,\ I_z\ [Nms^2]$ are the body frame inertia with respect to the corresponding axis, $g\ [m/s^2]$ is the gravitational constant, and $m\ [Kg]$ is the total mass of the quadrotor. In Eq. (5), the notations $s\theta$, $c\theta$ denote $sin(\theta)$, $cos(\theta)$, respectively. The quantities defined by $\dot{z}^*$ and $\dot{\psi}^*$ are simple linear controllers, whereas θ^* and ϕ^* are the ADRC control variables to be designed and then sent as input set-points for AR.Drone 2.0 microcontroller board. The z and ψ dynamics in the ODEs of Eq. (5), represent the idealized models of the drone internal controllers.

4. CONTROL DESIGN

4.1 Proposed developments

For the present control problem, we adopt the scheme illustrated in Fig. 4.

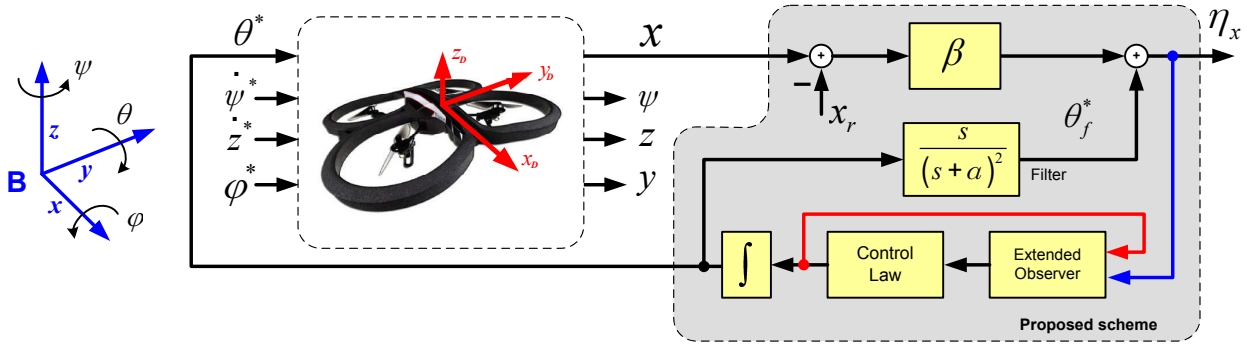

Figure 4: An illustrative diagram of the proposed control strategy. For simplicity, only the control loop for the state variable x is depicted in the diagram.

According to the mathematical formalism discussed in the previous section (Riveros *et al.*, 2017), (Zachi *et al.*, 2019) and based on the simplified diagram of Fig. 4, we apply the modified ADRC method to the dynamics of Eq. (5), by defining the output tracking errors as:

$$\eta_x = \beta(x - x_r) + \theta_f^*\,, \tag{6}$$

$$\eta_y = \beta(y - y_r) + \phi_f^*\,, \tag{7}$$

$$e_z = z - z_r\,, \qquad e_\psi = \psi - \psi_r\,, \tag{8}$$

in which $x_r,\ y_r,\ z_r,\ \psi_r\ \in \mathbb{R}$ are the reference position coordinates and the yaw angle for the drone, respectively, with respect to the base frame B. The quantities $\theta_f^*,\ \phi_f^*\ \in \mathbb{R}$ are the filtered versions of the desired control signals θ^* and

ϕ^*, respectively. The constants $\alpha,\ \beta \in \mathbb{R}$, seen in Fig. 4, are design parameters. Thus, in terms of the output errors, the system dynamics assumes the following format:

$$\ddot{\eta}_x + \gamma_1\dot{\eta}_x + \gamma_0\eta_x = g_x(t) \ + \ \dot{\theta}^* \,, \tag{9}$$

$$\ddot{\eta}_y + \gamma_1\dot{\eta}_y + \gamma_0\eta_y = g_y(t) \ + \ \dot{\phi}^* \,, \tag{10}$$

$$\dot{e}_z = \dot{z} - \dot{z}_r \,, \qquad \dot{e}_\psi = \dot{\psi} - \dot{\psi}_r \,. \tag{11}$$

where we define the *total disturbance terms* $g_x,\ g_y$ which gather together all the unmeasurable signals and uncertainties of the resulting dynamics. After the design constant $\alpha > 0$ of the filters in Fig. 4 is chosen conveniently, then we will have a stable polynomial given by $(s+\alpha)^2 = s^2 + \gamma_1 s + \gamma_0$, from which we can assert the stability of the left-hand side parts of the dynamics in Eqs. (9), (10). However, since the disturbance terms $\hat{g}_x,\ \hat{g}_y$ are not measurable, then *Extended State Observers* (ESOs) are employed for estimating such signals. The ESOs designs follow from the state space representations of the error systems in (9), (10) that is, with $\xi_x = [\eta_x,\ \dot{\eta}_x,\ g_x]^T$ and $\xi_z = [\eta_y,\ \dot{\eta}_y,\ g_y]^T$ as state vectors. As a standard approach, the ESOs assume the following formats:

$$\dot{\hat{\xi}}_x = \begin{bmatrix} 0 & 1 & 0 \\ -\gamma_0 & -\gamma_1 & 1 \\ 0 & 0 & 0 \end{bmatrix} \hat{\xi}_x + \begin{bmatrix} 0 \\ 1 \\ 0 \end{bmatrix} \dot{\theta}^* + L(\xi_{x1} - \hat{\xi}_{x1}) \,, \qquad \hat{\xi}_{x1} = [1\ 0\ 0]\hat{\xi}_x \,, \tag{12}$$

$$\dot{\hat{\xi}}_y = \begin{bmatrix} 0 & 1 & 0 \\ -\gamma_0 & -\gamma_1 & 1 \\ 0 & 0 & 0 \end{bmatrix} \hat{\xi}_y + \begin{bmatrix} 0 \\ 1 \\ 0 \end{bmatrix} \dot{\phi}^* + L(\xi_{y1} - \hat{\xi}_{y1}) \,, \qquad \hat{\xi}_{y1} = [1\ 0\ 0]\hat{\xi}_y \,, \tag{13}$$

$$L = [L_1,\ L_2, L_3]^T \,, \qquad (s+w_0)^3 = s^3 + L_1 s^2 + L_2 s + L_3 \,, \quad w_0 > 0 \in \mathbb{R}, \,. \tag{14}$$

in which, L is the vector of constant gains for the ESOs that are chosen to satisfy the coefficients of a stable polynomial (14) with multiple roots at $s = -w_0$. Thus, by ADRC Theory (Madoński *et al.*, 2015), (Zachi *et al.*, 2019), if the positive constant w_0 is chosen as a sufficiently large value, then the ESO estimated signals become very close to the real signals. So, the control variables in (9) and (9) can be implemented directly from (12) and (13), by computing:

$$\dot{\theta}^* = -\hat{g}_x(t) = -\hat{\xi}_{x3} \quad \longrightarrow \quad \theta^* = -\int \hat{\xi}_{x3}(t)dt \,, \tag{15}$$

$$\dot{\phi}^* = -\hat{g}_y(t) = -\hat{\xi}_{y3} \quad \longrightarrow \quad \phi^* = -\int \hat{\xi}_{y3}(t)dt \,, \tag{16}$$

$$\dot{z}^* = -K_z[z - z_r] \,,\ K_z > 0 \,, \qquad \dot{\phi}^* = -K_\psi[\psi - \psi_r] \,,\ \ K_\psi > 0. \tag{17}$$

5. SIMULATION RESULTS

In order to illustrate the efficiency of the proposed ADRC strategy for dealing with parametric uncertainties of the plant and also with the unmodeled dynamics, simulation results are presented. For coding the AR.Drone 2.0 equations in the Simulink environment, we use the complete description of its dynamics and parameters reported in (Merheb *et al.*, 2017). We use the feedback linearization technique applied to each drone state variable to construct and thus emulate the internal controller. For performing the joystick commands, we use the control laws in Eqs. (15)-(17) together with the ESOs in Eqs. (12)-(13). The reference trajectory adopted in the simulation trials is given by Eq. (18). Time delays of 0.5 seconds are also introduced in the measurements of the drone state variables together with an additive random noise of amplitude 0.01. The reason of introducing time delays in the simulations is an attempt to reproduce the real effect observed in the preliminary experimental tests with the vehicle. The simulation results obtained are shown in Fig. 5.

$$x_r(t) = cos\,(2\pi t/25)\ [m] \,, \quad y_r(t) = sin\,(2\pi t/25)\ [m] \,, \quad z_r(t) = 0.8\,[m] \,, \quad \psi_r(t) = 0^\circ \,. \tag{18}$$

The parameter used in the simulator blocks are: $w_0 = 800$, $\beta = 0.25$, $\gamma_1 = 0.2$, $\gamma_0 = 0.01$, $m = 0.429\ Kg$, $I_x = 0.00223\ Nms^2$, $Iy = 0.00298\ Nms^2$, $Iz = 0.0048\ Nms^2$. In simulations results, the closed loop system reveals good steady state tracking performance. It is important to mention that by increasing the value of parameter w_0, the ESO estimation becomes more precise. However, it is not recommended to choose excessive large values when measurement noise is presented.

6. EXPERIMENTAL RESULTS

In this section, experimental results are presented to illustrate the performance of the proposed ADRC controllers. For the experimental trials, we use a LabView AR.Drone 2.0 Toolkit Application program which is capable of establishing wi-fi communication with the drone control board for capturing sensor data and send flight commands. The proposed ADRC automatic controller, which is composed by the parallel filter of Fig. 4, the control laws of Eqs. (15)-(17) and the ESOs, is implemented using block-type code within LabView environment, running at $5\ ms$. The reference trajectory is given by Eq. (18). The obtained results are depicted in Fig. 6.

As can be seen from Fig. 6, the reference trajectory is achieved with small errors and with a time delay of approximately $0.5\ s$, which is possibly due to the wi-fi link between AR.Drone 2.0 control board and the LabView Toolkit program. In this case, such time delay was not sufficient for generating system instability. Notice from Eqs. (15)-(17) that the only information needed for generating the control laws θ^* and ϕ^* are the ESO state estimates $\hat{g}_x(t)$ and $\hat{g}_y(t)$, respectively. Since those estimates are not dependent on system parameters and unsearurable signals, then the proposed ADRC strategy does not require the exact knowledge of plant model, which is an attractive and desired robustness property.

7. CONCLUSIONS AND FUTURE WORKS

This work proposed a control solution for the problem of flight automatization commands of a quadrotor-type Unmanned Aerial Vehicle (AUV). The idea of the work was to apply an extension of the Active Disturbance Rejection

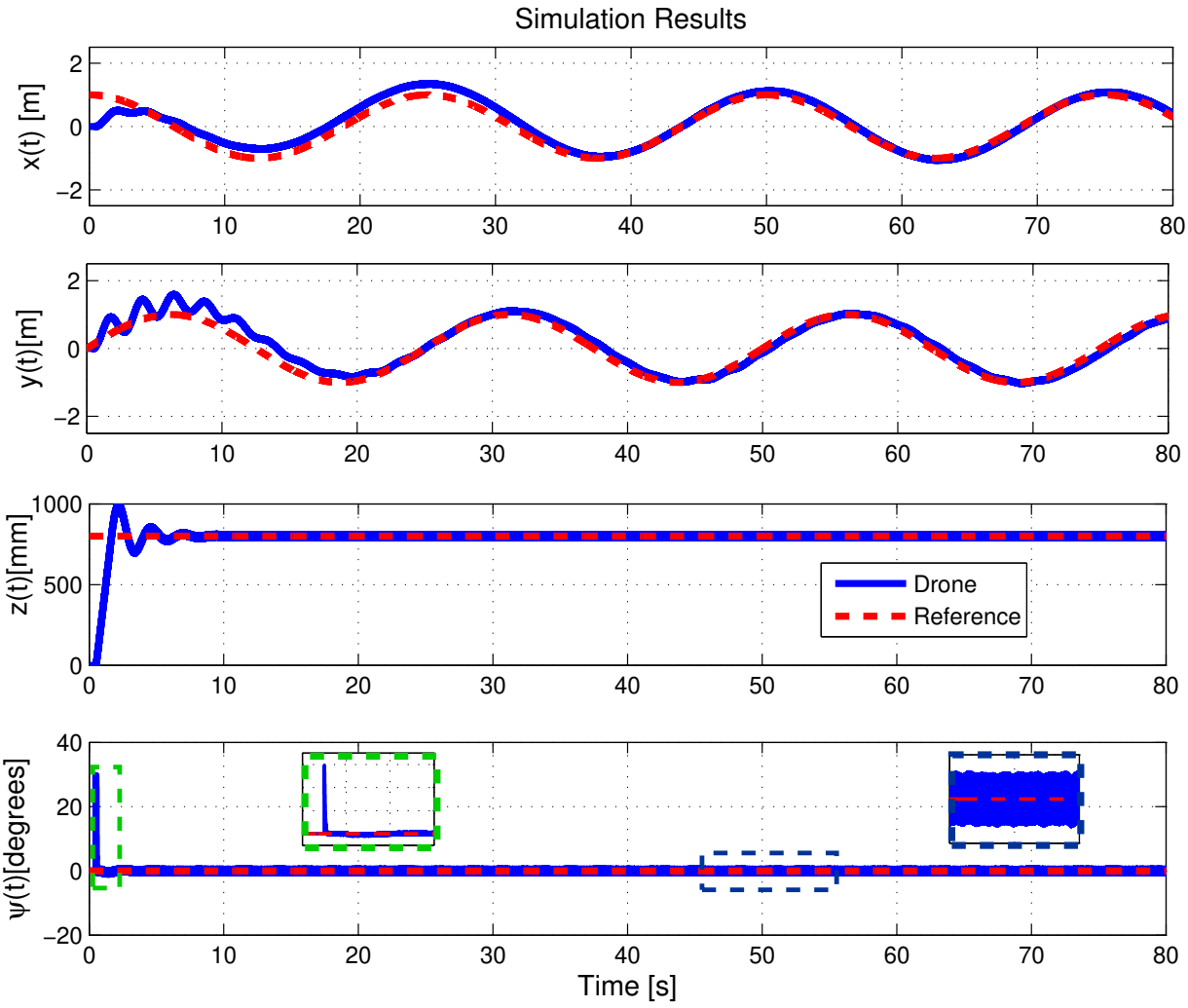

Figure 5: Simulation results obtained with the proposed ADRC strategy.

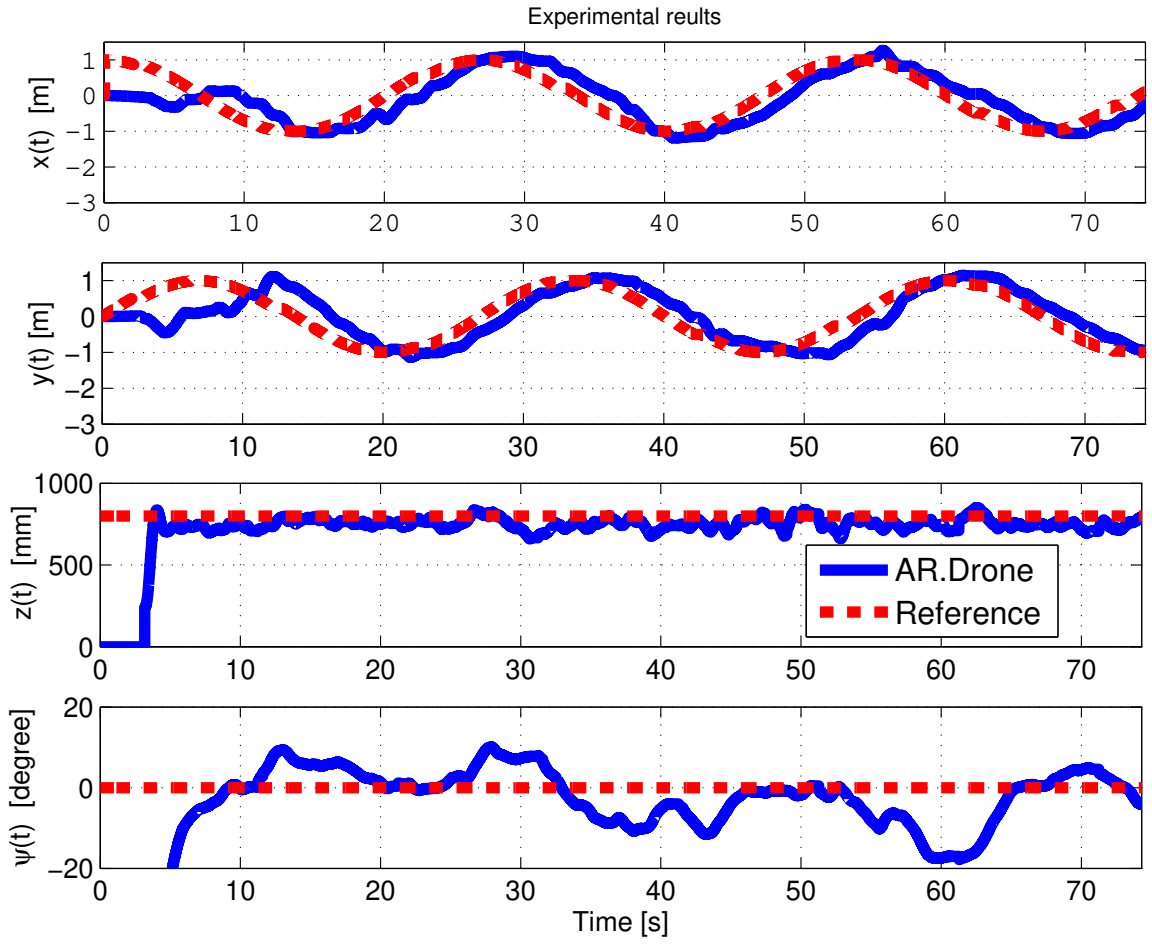

Figure 6: Experimental results obtained with the proposed ADRC strategy.

Control (ADRC) method to deal with the uncertainties and unmodeled dynamics of the plant. For solving the problem of output tracking control applied to Drone uncertain plant, a recently proposed modified version of the ADRC method was used. The main advantage of the modified ADRC framework when compared to the basic version is the lack of requirement on the knowledge of the control coefficient b, which is needed in the former. Simulation results were performed to illustrate the performance of the closed loop system numerically. Such results revealed a very close performance behavior when compared to the experimental results obtained in a real AR.Drone 2.0 vehicle.

For future studies involving the *modified ADRC* method, investigations are being carried out toward its extension to the challenging case of plants with unknown control direction, i.e., when the control coefficient b has unknown sign. For this case, the design and theoretical demonstrations reported in the literature for the method, both need to be reviewed.

8. REFERENCES

Babu, V.M., Das, K. and Kumar, S., 2017. "Designing of self tuning PID controller for AR drone quadrotor". In *2017 18th international conference on advanced robotics (ICAR)*. IEEE, pp. 167–172.

Bednowitz, N., Batta, R. and Nagi, R., 2014. "Dispatching and loitering policies for unmanned aerial vehicles under dynamically arriving multiple priority targets". *Journal of simulation*, Vol. 8, No. 1, pp. 9–24.

Berni, J.A., Zarco-Tejada, P.J., Suárez, L. and Fereres, E., 2009. "Thermal and narrowband multispectral remote sensing for vegetation monitoring from an unmanned aerial vehicle". *IEEE Transactions on Geoscience and Remote Sensing*, Vol. 47, No. 3, pp. 722–738.

Bristeau, P.J., Callou, F., Vissiere, D. and Petit, N., 2011. "The navigation and control technology inside the AR. Drone micro uav". *IFAC Proceedings Volumes*, Vol. 44, No. 1, pp. 1477–1484.

Feng, Z., Guan, N., Lv, M., Liu, W., Deng, Q., Liu, X. and Yi, W., 2017. "Efficient drone hijacking detection using onboard motion sensors". In *Design, Automation & Test in Europe Conference & Exhibition (DATE), 2017*. IEEE, pp. 1414–1419.

Guo, B., Bacha, S. and Alamir, M., 2017. "A review on adrc based pmsm control designs". In *Industrial Electronics Society, IECON 2017-43rd Annual Conference of the IEEE*. IEEE, pp. 1747–1753.

Han, J., 2009. "From PID to active disturbance rejection control". *IEEE transactions on Industrial Electronics*, Vol. 56, No. 3, pp. 900–906.

Hernandez, A., Murcia, H., Copot, C. and De Keyser, R., 2015. "Towards the development of a smart flying sensor: illustration in the field of precision agriculture". *Sensors*, Vol. 15, No. 7, pp. 16688–16709.

Kim, J., Kang, M.S. and Park, S., 2009. "Accurate modeling and robust hovering control for a quad-rotor VTOL aircraft". In *Selected papers from the 2nd International Symposium on UAVs, Reno, Nevada, USA June 8–10, 2009*. Springer, pp. 9–26.

Kim, K., Hyun, J. and Myung, H., 2017. "Development of aerial image transmitting sensor platform for disaster site surveillance". In *2017 17th International Conference on Control, Automation and Systems (ICCAS)*. IEEE, pp. 794–796.

Kim, S.J., Jeong, Y., Park, S., Ryu, K. and Oh, G., 2018. "A survey of drone use for entertainment and AVR (augmented and virtual reality)". In *Augmented Reality and Virtual Reality*, Springer, pp. 339–352.

Lee, W.K. and Song, K.M., 2018. "Enhanced ISAR imaging for surveillance of multiple drones in urban areas". In *2018 International Conference on Radar (RADAR)*. IEEE, pp. 1–4.

Madoński, R., Gao, Z. and Łakomy, K., 2015. "Towards a turnkey solution of industrial control under the active disturbance rejection paradigm". In *54th Annual Conference of the Society of Instrument and Control Engineers of Japan (SICE)*. IEEE, pp. 616–621.

Máthé, K., Buşoniu, L., Barabás, L., Iuga, C.I., Miclea, L. and Braband, J., 2016. "Vision-based control of a quadrotor for an object inspection scenario". In *2016 International Conference on Unmanned Aircraft Systems (ICUAS)*. IEEE, pp. 849–857.

Merheb, A.R., Noura, H. and Bateman, F., 2017. "Emergency control of AR Drone quadrotor UAV suffering a total loss of one rotor". *IEEE/ASME Transactions on Mechatronics*, Vol. 22, No. 2, pp. 961–971.

Riveros, S.R.D., Lima, P.P.P., Zachi, A.R.L. and Gouvêa, J.A., 2017. "Visual servoing stabilization of a ball and plate mechanism by using an enhanced disturbance rejection control method". In *24th ABCM International Congress of Mechanical Engineering (COBEM2017)*. December, 3th-8th, Curitiba, PR, Brazil. Associação Brasileira de Engenharia e Ciências Mecânicas - ABCM.

Xia, A., Hu, G., Li, Z., Huang, D. and Wang, F., 2018. "Self-optimizing pitch control for large scale wind turbine based on adrc". In *IOP Conference Series: Materials Science and Engineering*. IOP Publishing, Vol. 301, pp. 1–8.

Xia, Y., Pu, F., Li, S. and Gao, Y., 2016. "Lateral path tracking control of autonomous land vehicle based on ADRC and differential flatness". *IEEE Transactions on Industrial Electronics*, Vol. 63, No. 5, pp. 3091–3099.

Yin, X., Lan, Y., Wen, S., Zhang, J. and Wu, S., 2018. "Natural UAV tele-operation for agricultural application by using Kinect sensor". *International Journal of Agricultural and Biological Engineering*, Vol. 11, No. 4, pp. 173–178.

Zachi, A., Correia, C.A., Luiz Filho, J. and Gouvea, J., 2019. "Robust disturbance rejection controller for systems with uncertain parameters". *IET Control Theory & Applications*. doi:10.1049/iet-cta.2018.5291.

Zheng, Q., Dong, L., Lee, D.H. and Gao, Z., 2008. "Active disturbance rejection control for MEMS gyroscopes". In *American Control Conference, 2008*. IEEE, pp. 4425–4430.

Zheng, Q., Gaol, L.Q. and Gao, Z., 2007. "On stability analysis of active disturbance rejection control for nonlinear time-varying plants with unknown dynamics". In *Decision and Control, 2007 46th IEEE Conference on*. IEEE, pp. 3501–3506.